



**HAL**  
open science

## **Artificial weathering of plastics used in oyster farming**

Marion Hingant, Stéphanie Mallarino, Egle Conforto, Emmanuel Dubillot, Pierrick Barbier, Arno Bringer, Hélène Thomas

► **To cite this version:**

Marion Hingant, Stéphanie Mallarino, Egle Conforto, Emmanuel Dubillot, Pierrick Barbier, et al. Artificial weathering of plastics used in oyster farming. *Science of the Total Environment*, 2023, 868, pp.161638. <10.1016/j.scitotenv.2023.161638>. <hal-04371883>

**HAL Id: hal-04371883**

**<https://hal.science/hal-04371883v1>**

Submitted on 22 Jan 2024

**HAL** is a multi-disciplinary open access archive for the deposit and dissemination of scientific research documents, whether they are published or not. The documents may come from teaching and research institutions in France or abroad, or from public or private research centers.

L'archive ouverte pluridisciplinaire **HAL**, est destinée au dépôt et à la diffusion de documents scientifiques de niveau recherche, publiés ou non, émanant des établissements d'enseignement et de recherche français ou étrangers, des laboratoires publics ou privés.



HAL Authorization

# 1 **Artificial weathering of plastics used in oyster farming**

2

3 Marion Hingant <sup>1+</sup>, Stéphanie Mallarino <sup>2</sup>, Egle Conforto <sup>2</sup>, Emmanuel Dubillot <sup>1</sup>, Pierrick Barbier <sup>4</sup>,

4 Arno Bringer <sup>1,3\*</sup>, Hélène Thomas <sup>1\*</sup>

5 <sup>1</sup> Littoral Environnement et Sociétés (LIENSs), UMRi 7266 CNRS - La Rochelle Université, 2 rue  
6 Olympe de Gouges, F-17042 La Rochelle Cedex 01, France.

7 <sup>2</sup> Laboratoire des Sciences de l'Ingénieur pour l'Environnement (LaSIE), UMR 7356 CNRS – La  
8 Rochelle Université, Avenue Michel Crépeau, 17042 La Rochelle, France.

9 <sup>3</sup> Qualyse, 5 Allée de l'Océan, 17000 La Rochelle, France.

10 <sup>4</sup> Centre pour l'Aquaculture, la Pêche et l'Environnement de Nouvelle-Aquitaine (CAPENA), Prise de  
11 Terdoux, 17480 Le Château d'Oléron, France.

12 <sup>+</sup>: Corresponding author: Marion Hingant: Tel: +33 6 59 90 62 15 (FR), [marion.hingant@univ-lr.fr](mailto:marion.hingant@univ-lr.fr)

13 <sup>\*</sup>: Equal contribution

14

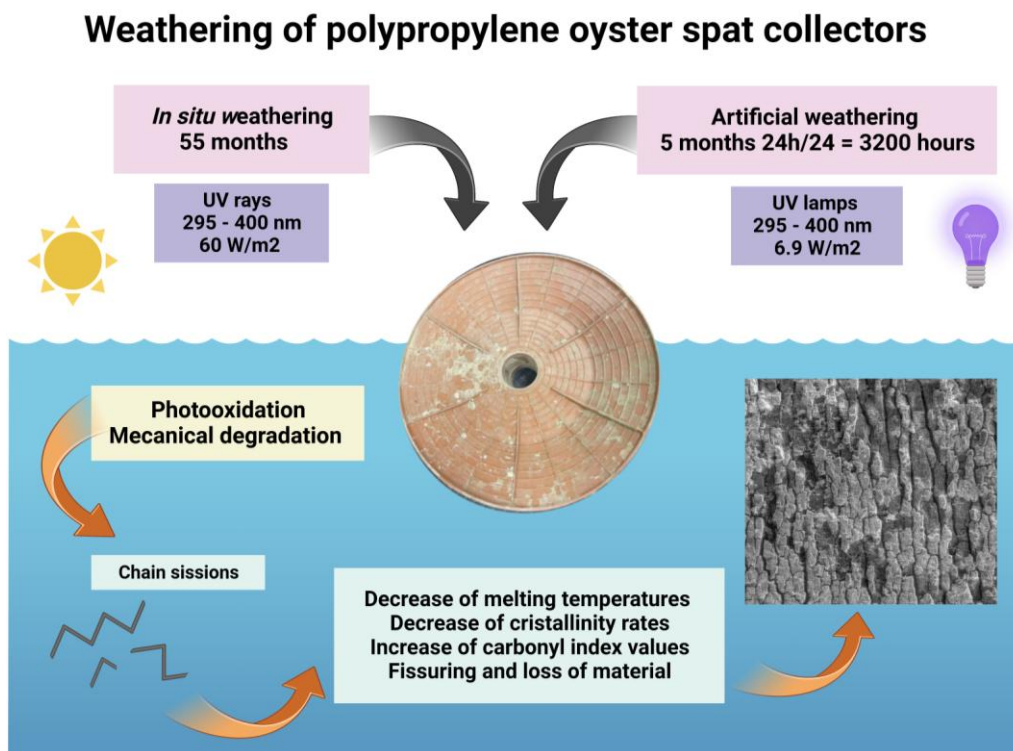
## 15 **ABSTRACT**

16 With the omnipresence of plastic litter from oyster farming in marine coastal areas, the objective of  
17 this work was to better understand the weathering of plastics used in this field, focusing on oyster spat  
18 collectors. During their use, around fifteen years, collectors made of polypropylene (PP) undergo  
19 numerous degradations, alternatively submerged, emerged in seawater, and stored outdoor until the  
20 next cycle. They weaken, crack, break, end up fragmenting and disseminated in the environment as  
21 microplastics associated to persistent organic pollutants. In this work, a comparison of 55 months of *in*  
22 *situ* weathering with five months of artificial weathering in air or in artificial seawater in a homemade  
23 UV chamber was conducted to better understand the mechanisms involved. Chemical, thermal and  
24 surface characterizations of virgin and weathered samples were conducted using Fourier Transform  
25 Infrared Spectroscopy (FTIR), Differential Scanning Calorimetry (DSC) and Environmental Scanning  
26 Electron Microscopy (ESEM). After 55 months of *in situ* weathering, collectors were notably  
27 damaged with large fissures and loss of microplastics (MPs) associated with an increase of carbonyl

28 index values and a decrease of melting temperatures and crystallinity rates. Considering only UV  
29 irradiation, five months of artificial weathering at 30°C under continuous irradiation of 6.9 W/m<sup>2</sup>  
30 under UV lamps (295 - 400 nm) reproduced approximately 4.4 months of natural sunlight. Artificial  
31 weathering confirmed that photooxidation by combined effects of UV rays and oxygen was the main  
32 weathering mechanism and was reduced in seawater. These results help to understand the mechanisms  
33 involved in the weathering of these collectors in the marine environment and provide valuable  
34 informations for industrials and professionals. Our study suggests a better storage away from UV rays  
35 and a reduction of the duration of use compared to current practices.

36

### 37 GRAPHICAL ABSTRACT



38

### 39 KEYWORDS

40 Oyster farming, Polypropylene, Photooxidation, *In situ* weathering, Artificial weathering

### 41 ABBREVIATIONS

42 PP : Polypropylene, MPs : Microplastics, POPs : Persistent organic pollutants

43

## 44 1. INTRODUCTION

45 At now, a total of five ocean gyres with high concentrations of plastics debris have been identified  
46 (Avio *et al.*, 2017; Law *et al.*, 2010). 80 % of these marine debris are land-based sources and 20 %  
47 are ocean-based sources like fisheries and maritime activities (Avio *et al.*, 2017; Bringer *et al.*,  
48 2021b). Since the arrival of plastic from petrochemicals in the 1950s, professionals in aquaculture  
49 activities have progressively turned to this new material, which is more resistant, durable, and  
50 economical. Due to their stability, plastics persist in the environment for hundreds of years (Cai *et*  
51 *al.*, 2018; Gewert *et al.*, 2015a). Degradation of plastics can proceed by chemical, physical  
52 degradations and biological degradations (Gewert *et al.*, 2015; Singh and Sharma, 2008; Song *et al.*,  
53 2017). Degradation rates are dependent on the manufacturing process (Han *et al.*, 2018), the presence  
54 of stabilizers, additives and the weathering conditions including sunlight, temperature, and mechanical  
55 stress (Avio *et al.*, 2017a; Kalogerakis *et al.*, 2017a; Masry *et al.*, 2021a; Rajakumar, Sarasvathy,  
56 Thamarai Chelvan, *et al.*, 2009). In seawater, degradation rates are lower and more uniform compared  
57 to landfill due to lower and less variable conditions as UV irradiation, oxygen content and  
58 temperatures (Cai *et al.*, 2018; Gewert *et al.*, 2015). But in any cases, degradations finally lead to the  
59 release of microplastics (MPs) in the environment which can be accumulated by a wide range of  
60 marine organisms from zooplankton (Cole *et al.*, 2013), to fishes through bivalves (Bringer *et al.*,  
61 2021a) being transferred along food chains until humans (Avio *et al.*, 2017a). Some studies have  
62 reported the presence of MPs in human organs (Hermabessiere *et al.*, 2017), blood (Leslie *et al.*, 2022)  
63 and faeces (Zhang *et al.*, 2021). MPs exposure by ingestion, inhalation or dermal contact can cause  
64 physical damages, with oxidative stress, or inflammatory lesions (Prata *et al.*, 2020).

65  
66 Furthermore, plastics are associated with additives and stabilizers (Zhang *et al.*, 2021). Plasticizers as  
67 di-n-butyl phthalate, antioxidant agents as bisphenol A, flame retardants as tris-2-chloro-éthyl  
68 phosphate, are chemicals added during the manufacturing process to obtain certain desired properties  
69 (Avio *et al.*, 2017a; Masry *et al.*, 2021a). Because they are usually not covalently bonded to the  
70 polymers (Gewert *et al.*, 2015; Paluselli *et al.*, 2019; Wang *et al.*, 2020), these chemicals can migrate

71 from the polymeric matrix towards the surrounding environment. In seawater, leaching of these  
72 chemicals by diffusion is dependent on their solubility, their polarity, and their affinity to the matrix  
73 (Paluselli *et al.*, 2019). Some of these chemicals are known to be harmful to the marine ecosystems and  
74 humans causing dysfunctions of the immune and reproductive systems, cancers and neurodegenerative  
75 disorders (Avio *et al.*, 2017; Hermabessiere *et al.*, 2017).

76

77 Plastics are also able to absorb various pollutants called persistent organic pollutants (POPs) present in  
78 the marine environment such as pesticides as dichlorodiphenyltrichloroethane, polycyclic  
79 hydrocarbons as naphthalene, and heavy metals as cadmium and lead for examples (Boucher *et al.*,  
80 2016; Gewert *et al.*, 2015; Hermabessiere *et al.*, 2017; Holmes *et al.*, 2012; León *et al.*, 2018; Paluselli  
81 *et al.*, 2019). These pollutants can be ingested and bioaccumulated by marine organisms and humans,  
82 often vectorized by MPs (Avio *et al.*, 2017; Gewert *et al.*, 2015; Guo and Wang, 2019; Prata *et al.*,  
83 2020). The risks that MPs and these persistent organic pollutants (POPs) pose to marine life and  
84 humans are widely recognized and have been included in national and international marine protection  
85 strategies, policies, and legislation (EU Marine Strategy Framework Directive).

86

87 With nearly 30,000 tons of Pacific oysters *Crassostrea gigas* produced each year, the department of  
88 Charente-Maritime in France represents the first French production area with one third of the national  
89 production (AGRESTE 2019). Different types of plastics such as polypropylene (PP), polyethylene  
90 (PE) and polyvinyl chloride (PVC) are now used at each stage of production. Oyster spat collection is  
91 the first phase of production in traditional oyster farming. Collectors have a specific design of a disc of  
92 160 mm diameter, slightly concave, flexible and ribbed, with a thickness of 0.6 mm, designed in order  
93 to collect a maximum of oyster spats in seawater during the reproductive period between July and  
94 March. After collecting, collectors are taken out of seawater, oysters are detached and then transferred  
95 to oyster bags. The environmental image of the profession is criticized today given the omnipresence  
96 of plastic waste from oyster farming in coastal areas. Around 200 tons of plastic waste from oyster  
97 farming, including 60 tons of oyster spat collectors, are found each year in the Atlantic south coast

98 (FEAMP 2020). During their use around fifteen years, collectors made of PP or PE undergo numerous  
99 degradations. They weaken, crack, break, end up fragmenting, disseminating MPs and chemicals in  
100 the marine environment. The toxicity of weathered MPs and associated chemicals from oyster farming  
101 was recently evaluated on early stages of bivalve development (Bringer, Cachot, *et al.*, 2021).  
102 Diméthylphtalate used as plasticizer and naphthalene as polycyclic hydrocarbons absorbed in the  
103 marine environment have been identified on weathered oyster crops, collectors, and pipes (Bringer, Le  
104 Floch, *et al.*, 2021) . Faced with the growing risk associated to plastics used in oyster farming for  
105 marine life and humans, it is necessary understand and reduce their anthropogenic impacts.

106

107 *In situ* and artificial weathering of PP have been described in many studies (Badji *et al.*, 2018a; Lv *et*  
108 *al.*, 2015; Rajakumar, Sarasvathy, Thamarai Chelvan, *et al.*, 2009; Tang *et al.*, 2019a) but were never  
109 established for PP oyster spat collectors. These collectors are interesting because they have a chemical  
110 composition and mechanical properties, with additives and stabilizers designed for aquaculture  
111 activities specifications and because, *in fine*, oysters are destined for human consumption. In this  
112 work, a comparison of 55 months *in situ* weathering with five months of artificial weathering in a  
113 homemade UV chamber was conducted to better understand the mechanisms involved in PP collectors  
114 degradations. With the aim of understanding the mechanisms of degradation of these collectors in the  
115 marine environment, chemical, thermal, and structural characterizations of virgin and weathered  
116 collectors were performed using Environmental Scanning Electron Microscopy (ESEM), Differential  
117 Scanning Calorimetry (DSC), and Fourier Transform Infrared Spectroscopy (FTIR).

118

## 119 **2. MATERIALS AND METHODS**

### 120 ***2.1 Oyster collectors***

#### 121 ***2.1.1 In situ weathering***

122 In 2017, a project conducted by the Center for Aquaculture, Fisheries, and the Environment of  
123 Nouvelle-Aquitaine (CAPENA) had the objective to compare petrosourced and biosourced collectors  
124 in terms of oyster spat collection efficiencies. Collectors have a specific design of a disc of 160 mm

125 diameter, slightly concave, flexible and ribbed, with a thickness of 0.6 mm. These collectors were  
126 immersed in the area of the Pertuis Charentais, in the French department Charente-Maritime  
127 (45°51'41.7"N 1°12'19.0"W) during three cycles of eight months collecting oyster spats in seawater  
128 between 2017 and 2020. These collectors were alternatively submerged and emerged in seawater  
129 during collection and were stored outdoors until the next collection cycle. Each cycle started in July  
130 and stopped in March. In total, these collectors spent 24 months in seawater, and 31 months stored  
131 outdoors until the start of this work in January 2022. A continuous environmental monitoring during  
132 *in situ* weathering measured seawater temperature from 6 to 21 °C, salinity from 26 to 34 g/L,  
133 outdoor temperature from 5 °C to 23 °C and a mean solar irradiance of 1200 kW/h/m<sup>2</sup>/year. Virgin  
134 collectors, as references, were stored indoors and protected from humidity and UV rays. Virgin and *in*  
135 *situ* weathered collectors were characterized by FTIR, DSC, and ESEM as described below.

136

### 137 **2.1.2 Artificial weathering**

138 Inspired by ISO 4892:2016 part 3 and ATSM G154:06, a homemade UV chamber was equipped with  
139 five UV lamps with wavelength between 295 and 400 nm (KFMS reference PH710932 15W). These  
140 UV lamps were selected because they can give a good reproduction of natural sunlight in the UV  
141 range (Andrade *et al.*, 2019; Cai *et al.*, 2018) and because this medium energy is particularly efficient  
142 in facilitating photodegradation of PP (Andrady, 2015). Virgin PP collectors were weathered under  
143 UV rays in two different conditions: in air (UV+) or immersed in artificial seawater at 30 g/L  
144 (UV+/SW). Negative controls, not exposed to UV rays, were installed in a box in the chamber (UV-  
145 and UV-/SW). Artificial seawater was made by mixing milliQ water and commercial salt. Virgin PP  
146 collectors were installed directly under UV lamps at 15 cm (UV+) or in borosilicate crystallizers filled  
147 with 500 mL of 30 g/L of artificial seawater (SW) and closed with a borosilicate lid to limit  
148 evaporation but letting pass UV rays through. This experiment was conducted for five months, at  
149 30°C, under 24h/24 continuous UV irradiation. Temperature was monitored weekly with a mercury  
150 thermometer. Intensity was monitored weekly with a radiometer (RS Pro reference IM-213) placed at  
151 15 cm from the lamps and was approximately equal to 6.9 W/m<sup>2</sup> in a empty crystallizer and 3 W/m<sup>2</sup> in

152 artificial seawater. Salinity was monitored weekly with a multiparameter (WMW reference Multi3430  
153 with Tetracon 925 probe) and was adjusted to 30 g/L by adding milliQ water if necessary. Each  
154 month, one triplicate for each condition was removed and stored in glass petri dishes at 4 °C, in the  
155 dark, to stop weathering.

156

## 157 ***2.2 Characterization***

### 158 ***2.2.1 Environmental Scanning Electron Microscopy (ESEM)***

159 The scanning electron microscope used in this work is an Environmental FEI Quanta 200 –  
160 ESEM/FEG (LaSIE, La Rochelle University) working at 9 KV of electron beam accelerating voltage  
161 and 0.1 nA of beam current under 200 Pa of water vapor pressure in the specimen chamber (Conforto  
162 *et al.*, 2015). Secondary electron-type images, providing topographical information from the surfaces,  
163 were obtained in environmental mode using a “Gaseous Large-Field” detector. The low-energy beam  
164 and environmental conditions used are necessary to observe plastic materials, which are thermally  
165 sensitive and poor electrical and thermal conductors, without any preparation. In fact, if a surface  
166 metallization (which is part of the sample preparation procedure) was performed, it could partially or  
167 totally mask cracks. The latter are an important parameter used to evaluate the weathering of plastic.  
168 Surface topography of different parts of virgin and weathered collectors was observed. We made sure  
169 that the results were coherent, homogenous, reproducible. Ten fissures lengths were measured on  
170 random fissures and averaged with FIJI software.

171

### 172 ***2.2.2 Fourier Transform Infrared Spectroscopy (FTIR)***

173 In order to identify the different types of chemical bonds, FTIR was used. Infrared frequency identical  
174 to the vibrational frequency of a bond results in absorption, creating a spectrum acting as a molecular  
175 “fingerprint” of the sample. The position, shape, and intensity of peaks in the spectrum reveal details  
176 about the molecular structure of the sample. Different parts of virgin and weathered collectors were  
177 analyzed using a thermoscientific Nicolet iS50 FTIR spectrophotometer equipped with an attenuated  
178 total reflectance mode (ATR). We made sure that the results were coherent, homogenous,

179 reproducible. Each spectrum was recorded as the average of 32 scans in the spectral range of 500 to  
180 4000  $\text{cm}^{-1}$ , with a spectral resolution at 4.0  $\text{cm}^{-1}$ . Ten spectras were done randomly at the surface of  
181 each sample averaged with a corrected baseline, and analyzed with Spectragryph 1.2 software.

182

### 183 **2.2.3 Differential Scanning Calorimetry (DSC)**

184 Specific temperatures of the samples such as melting temperature and crystallization, as well as the  
185 enthalpy values associated with these phenomena were examined on a differential scanning  
186 calorimeter TA Instrument Q100. Samples were cut, weighed, and heated from -60 °C to 210 °C in an  
187 aluminum pan, then cooled to 40 °C. All experiments were performed at a rate of 20 °C/min under  
188 nitrogen flow (50 ml/min) to avoid thermal degradation. For the sake of repeatability, at least two  
189 samples for each type of collector were used for the DSC measurements. The analysis of DSC  
190 thermograms was carried out with TA Universal Analysis software.

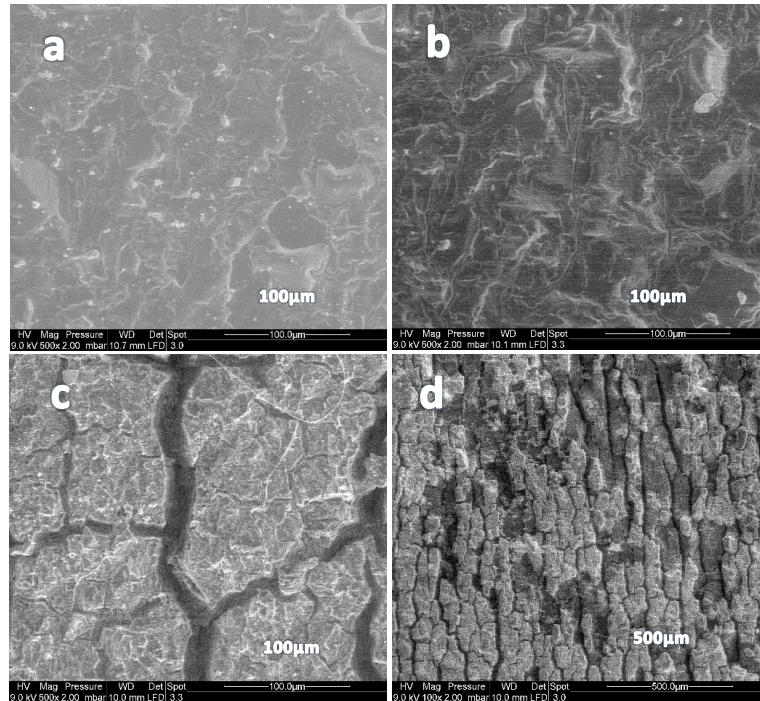
191

## 192 **3. RESULTS**

### 193 **3.1 Surface analysis**

194 Surface images were obtained by using environmental scanning electron microscopy (ESEM). Virgin  
195 PP collectors exhibited relatively homogeneous, smooth and compact textures without any fissures  
196 (Fig 1a). *In situ* weathered PP collectors (Fig 1c and 1d) exhibited heterogeneous surfaces, with large  
197 and deep averaged fissures up to 24  $\mu\text{m}$ . Loss of material was observed at lower magnification (Fig  
198 1d) caused by mechanical stress as tides, currents during submersion, wind and rain during emersion  
199 but also handling. This loss of material suggests a release of MPs in the environment. Crystals of  
200 sodium chloride salts and algae and diatom residues were also observed and confirmed that the  
201 collectors stayed in seawater. Artificially weathered collectors under UV rays (UV+) start fissuring  
202 after five months with the observation of 2  $\mu\text{m}$  length fissures (Fig 1b). No fissures were observed for  
203 the other conditions as negative control (UV-) and immersion in artificial seawater for five months  
204 (UV-/SW and UV+/SW) (Results not presented). Artificial weathering confirmed that fissuring started  
205 after five months exposed to UV rays.

206  
207  
208  
209  
210  
211  
212  
213  
214  
215  
216



217 Figure 1. ESEM pictures of (a) virgin PP collector x 500; (b) five months artificially weathered PP  
218 collector under UV rays x 500; (c) and (d) 55 months *in situ* weathered PP collector (x 500 and x 100  
219 respectively). Arrow point to a small fissure of 2  $\mu\text{m}$ .

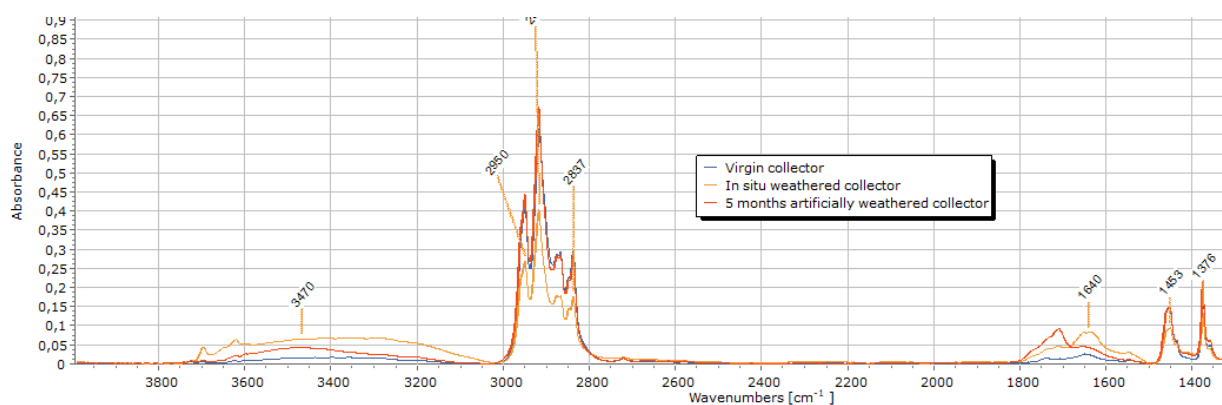
220  
221

### 3.2 Chemical analysis

222 The averaged infrared spectra of a virgin PP collector, used as reference, is presented in the Figure 2  
223 (blue). The spectra showed absorption peaks located at wavenumbers of 971, 995, 1167, 1375, 1454,  
224 2838, 2865, 2918, and 2953  $\text{cm}^{-1}$  corresponding to specific vibrations of rocking, bending and  
225 stretching and identified as the native hydrocarbon bonds of virgin PP ( $\text{C}_3\text{H}_6$ )<sub>n</sub> (Badji *et al.*, 2018b;  
226 Tang *et al.*, 2019b). Photooxidation, by combined effects of UV rays and oxygen, is known to be the  
227 main weathering process for thermoplastics such as PP (Andrady, 2015; Gewert, 2015; Kalogerakis *et*  
228 *al.*, 2017b; Masry *et al.*, 2021b). UV radiation has sufficient energy to break the C—C and C—H bonds  
229 (Singh & Sharma, 2008). Diminution of C—C and C—H bonds on the *in situ* weathered collector (Fig  
230 2 – orange) were observed at wavenumbers between 2800 - 3000  $\text{cm}^{-1}$  confirming their break. The free  
231 radicals produced during photooxidation reacted freely with atmospheric oxygen to form hydroxyl  
232 groups (O—H) peaking at wavenumbers between 3000 - 3700  $\text{cm}^{-1}$  and carbonyl groups (C=O)

233 including carboxylic acids and ketones peaking at wavenumber  $1711\text{ cm}^{-1}$ , esters and aldehydes  
234 peaking at wavenumber  $1740\text{ cm}^{-1}$  and lactones peaking at wavenumber  $1780\text{ cm}^{-1}$  (Badji *et al.*,  
235 2018a; Lv *et al.*, 2015; Masry *et al.*, 2021b). These new significant peaks at around wavenumbers  
236  $3000 - 3700\text{ cm}^{-1}$  and  $1500 - 1800\text{ cm}^{-1}$  were identifiable on *in situ* and artificially weathered collector  
237 infrared spectra (Fig 2) and their areas were a function of weathering conditions (Cai *et al.*, 2018;  
238 Rajakumar, Sarasvathy, Thamarai Chelvan, *et al.*, 2009; Tang *et al.*, 2019b).

239



240 Figure 2. FTIR spectra of a virgin PP collector (blue), *in situ* weathered PP collector (orange) and a 5  
241 months artificially weathered collector (UV+) (yellow)

242

243 The carbonyl index (CI) has been used to quantify the degree of weathering of various samples  
244 (Almond *et al.*, 2020; Badji *et al.*, 2018a; Julienne *et al.*, 2019; Rajakumar, Sarasvathy, Chelvan, *et*  
245 *al.*, 2009; Song *et al.*, 2017b; Tang *et al.*, 2019a). This index is defined as the ratio of the integrated  
246 area of the carbonyl group peak at around wavenumbers  $1700\text{ cm}^{-1}$  to an internal constant peak. In this  
247 work, boundaries between wavenumbers  $1390$  and  $1340\text{ cm}^{-1}$  were chosen for the constant peak  
248 because it remained unchanged during weathering. Consequently, boundaries between wavenumbers  
249  $1820$  and  $1570\text{ cm}^{-1}$  were chosen for the carbonyl peak. Carbonyl index of *in situ* and artificially  
250 weathered samples calculated on the average of ten spectra for each sample and after baseline  
251 correction are resumed in Table 1. Carbonyl index values for the virgin collector and negative control  
252 (UV-), as references, were similar and equal to 0.7 and 0.5 respectively. These values were not equal  
253 to zero probably due to thermal degradation of the material during injection. Negative control (UV-)

254 also confirmed that no additional degradation occurred during the five months of artificial weathering.  
255 Consequently, only UV ray exposure and immersion in seawater can be considered in this experiment.  
256 After five months of artificial weathering in seawater (UV-/SW), the carbonyl index value reached  
257 1.9. Additionally immersed and exposed to UV rays (UV+/SW), this value increased to 2.1. Finally,  
258 upon exposure to UV rays only during five months (UV+), the carbonyl index reached the value of 3.  
259 In this experiment, the highest value for carbonyl index was therefore found after five months  
260 artificially exposed to UV rays only (UV+). After 55 months of *in situ* weathering, the carbonyl index  
261 value reached 4.2.

262

### 263 **3.3 Thermal analysis**

264 Semi-crystalline PP has a heterogeneous structure, consisting of crystalline and amorphous phases  
265 (Masry *et al.*, 2021b). The crystallinity rate and the melting temperature are impacted by weathering  
266 (Badji *et al.*, 2018b). Monitoring the evolution of these parameters using Differential Scanning  
267 Calorimetry (DSC) gave a global indication of weathering degree of the samples. On the DSC  
268 thermograms (Fig 3), the heat flow exhibited endothermic peaks related to the melting of PP allowing  
269 the measure of melting temperatures and melting enthalpies ( $\Delta H_m$ ) corresponding to the energy needed  
270 to melt the sample. Crystallinity rates can be calculated as this relation: Crystallinity rate (%) =  $\Delta H_m /$   
271  $(\Delta H_{inf}) \times 100$  (equation 1) with  $\Delta H_{inf}$  equal to 209 J/g for PP corresponding to the theoretical melting  
272 enthalpy of a fully crystalline PP (Badji *et al.*, 2018; Han *et al.*, 2018)  $\Delta H_m$  can be calculated with TA  
273 analysis software. Melting temperatures and crystallinity rates and of virgin, *in situ* and artificially  
274 weathered PP collectors are summarized in Table 1. For the virgin collector, as reference, melting  
275 temperature was equal to 169 °C, melting enthalpy was equal to 59 J/g and crystallinity rate was equal  
276 to 29 % (equation 1). These values were equivalent for the negative control after five months of  
277 artificial weathering without UV rays (UV-). After *in situ* weathering, significant decreases of the  
278 melting temperature from 169 to 164 °C, and crystallinity rates from 29 to 25 % were observed.  
279 Changes in melting temperature and crystallinity rate were observed on samples exposed to UV rays  
280 (UV+). No differences were observed for the other conditions in seawater (UV+/SW, UV-/SW).

281  
 282  
 283  
 284  
 285  
 286  
 287  
 288  
 289  
 290  
 291  
 292  
 293

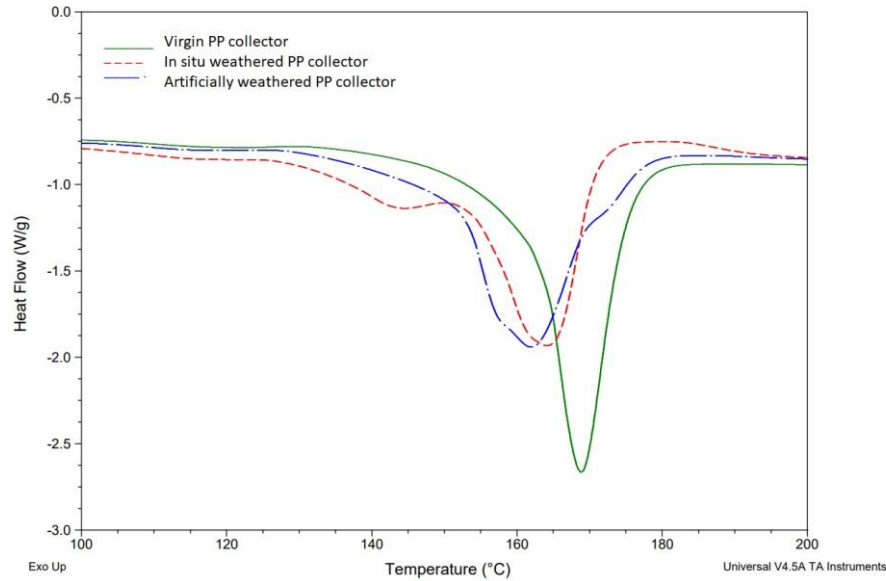


Figure 3. DSC thermograms of a virgin PP collector (green line), *in situ* weathered PP collector (red line) and artificially weathered PP collector (blue line) with endothermic peak indicating the melting of the material.

Virgin PP collector	55 months <i>in situ</i> weathered PP collector	5 month artificially weathered PP collectors			
		UV-	UV+	UV-/SW	UV+/SW
0.7	4.2	0.5	3.0	1.9	2.1
169	164	169	164	169	169
29	25	31	26	30	30
0	24	0	2	0	0

294  
 295  
 296  
 297  
 298

Table 1: Carbonyl index values, melting temperatures, crystallinity rates, and fissure lengths for virgin PP collectors, 55 months *in situ* weathered PP collectors, and five months artificially weathered PP collectors.

299 **4. DISCUSSION**

300 During their use, PP oyster spat collectors undergo various degradations as the result of  
 301 photooxidation, thermal degradation, mechanical degradation, and biodegradation, all based on free-

302 radicals mechanisms. (Avio *et al.*, 2017a; Singh & Sharma, 2008). After *in situ* weathering, increase  
303 of carbonyl index values, and decrease of crystallinity rates, melting temperatures and apparition of  
304 fissures were observed (Table 1). Artificial weathering was conducted to better understand the  
305 mechanisms involved. Because the temperature in the UV chamber was fixed, homogenous and  
306 relatively low, and because no additional mechanical stress was applied, only UV irradiation was  
307 considered in this experiment. The highest degradation rate obtained after UV irradiation in air  
308 (UV+) and negative control confirmed that no additional degradation than photooxidation occurred.  
309 Abiotic degradations precede biotic degradations. Photooxydation by combined effect of oxygen and  
310 UV rays is known to be the main weathering mecanisms for PP. Initiated by UV rays absorbed by  
311 structural abnormalities or impurities, photooxidation cause chain scissions and produce shorter and  
312 more mobile chains with free radicals reacting freely with atmospheric oxygen (Gewert *et al.*, 2015).  
313 This mechanism usually starts in the amorphous phase (Andrady, 2015; Julienne *et al.*, 2019a; Masry  
314 *et al.*, 2021, Han *et al.*, 2018) but results of this work obtained after artificial weathering showed a  
315 decrease of crystallinity rate indicating that photooxidation already caused damage in the amorphous  
316 phase and then occurred in the crystalline phase. This mechanism, already described by (Badji *et al.*,  
317 2018; Lv *et al.*, 2015; Tang *et al.*, 2019), finally lead to a decrease of the hydrophobicity and the  
318 molecular weigh of the polymer. However, the molecular weight remaining high, biodegradation of  
319 the long chains stays limited (Gewert *et al.*, 2015; Singh and Sharma, 2008). In fact, PP is often used  
320 as a negative control in biodegradation experiments (Kalogerakis *et al.*, 2017; Lott *et al.*, 2020).

321  
322 At the location of the *in situ* weathering, a mean solar irradiance of 1200 kWh/m<sup>2</sup>/year was monitored  
323 ([https://re.jrc.ec.europa.eu/pvg\\_tools/fr/#DR](https://re.jrc.ec.europa.eu/pvg_tools/fr/#DR)) which corresponds to an irradiance of 60 kWh/m<sup>2</sup>/year  
324 in the total UV range (295 and 400 nm). During artificial weathering, the intensity of the UV lamps in  
325 this same range was averaged at 6.9 W/m<sup>2</sup> and was maintained for 3200 hours which correspond to a  
326 total cumulated irradiance of 22 kWh/m<sup>2</sup> (= 6.9 x 3200). Consequently, artificial weathering  
327 reproduced approximately 134 days (22 / 60 x 365) corresponding to 4.4 months (Gewert *et al.*, 2018).

328 This calculation of solar simulation equivalent is theoretical because it is dependant of numerous  
329 environmental factors, which varies throughout the seasons.

330

331 After five months of artificial weathering in seawater, an increase of carbonyl index values was  
332 observed whereas the crystallinity rates and melting temperatures were little impacted (Table 1).  
333 Absorption of seawater in PP can allow the entrance of dissolved oxygen into the matrix favoring  
334 chain oxidation and hydrolysis (Kalogerakis *et al.*, 2017a) but the kinetics of these degradation  
335 mechanisms are slower than those for photooxidation. Moreover, intensity of UV irradiance in  
336 artificial seawater ( $3 \text{ W/m}^2$ ) was lower than for direct exposure to a UV lamp ( $6.9 \text{ W/m}^2$ ), reducing the  
337 photooxidation mechanism in seawater, wich it is expected to occur in the marine environment. No  
338 fissures were observed for these conditions (UV+/SW and UV-/SW).

339

340 Collectors artificially weathered during five months gave approximately the same results than after 55  
341 months weathered *in situ* except for the fissure lengths due to additional degradations involved *in situ*.  
342 It is important to consider that *in situ*, degradation of PP collectors was influenced by alternations of  
343 tides, day and night cycles, weather and seasonal conditions, presence of spats, biofooling and crystal  
344 salts. In conclusion, *in situ* weathering of these PP collectors was mainly caused by photooxidation  
345 during emersion and outdoor storage and was enhanced with additional effects of mechanical stresses  
346 such as tides, currents, wind and rain but also professional handling. Comparing *in situ* and artificial  
347 weathering must be done with caution since there is still not an adequate simulation of the combined  
348 effects and synergies of various environmental factors (Andrade *et al.*, 2019; Rajakumar,  
349 Sarasvathy, Thamarai Chelvan, *et al.*, 2009; Yang & Ding, 2006).

350

## 351 **5. CONCLUSIONS**

352 This is the first study comparing *in situ* and artificial weathering of PP oyster spat collectors. This  
353 work shows that after only 55 months *in situ*, alternatively submerged and emerged, the collectors  
354 were notably damaged, with large fissures and loss of material such as MPs. These damages were

355 mainly due to photooxidation during exposure to UV rays, enhanced by mechanical stress as tides,  
356 current, wind, rain and handling all along their use and storage. Considering only irradiation in the UV  
357 range, five months of artificial weathering reproduced approximately 4.4 months of natural sunlight *in*  
358 *situ* and confirmed that photooxidation by combined effect of UV rays and oxygen was the main  
359 weathering mechanism and was higher in air than in seawater. Degradations as the apparition of the  
360 first fissures were observed relatively soon under UV irradiation. This first comparative study gave  
361 preliminary results on this topic and help to better understand the mechanisms involved in the  
362 degradation of these collectors. This work allows to make recommendations to industrials and  
363 professionals including a better storage protected from UV rays and a reduction of the duration of use.  
364 It is important to note that there is still a lack of information on the toxicity and the potential  
365 environmental hazard of these altered plastics in the marine environment, as vectors of MPs, POPs and  
366 microorganisms (Avio *et al.*, 2017b; Gewert *et al.*, 2015b). Consequently, a future work will be  
367 focused on the relationship between weathering, fragmentation and toxicity including promising  
368 alternatives such as biosourced materials.

369

#### 370 **Funding and acknowledgements:**

371 The PLASTIC LAB project (Dégradabilité, effets et comportement des PLASTIques Conchylicoles en  
372 LABoratoire), was funded by the FEAMP (Fonds Européen des Affaires Maritimes et de la Pêche)  
373 and the SCIC TEO (Taho'E Eco Organisation). The authors thank the CAPENA, and Pierrick Barbier,  
374 for providing the oyster collectors used in this work, Latta Socciligame and Fanon Julienne for their  
375 help. The authors are gratefull to all contributors including Linda Sperling for their proofreading  
376 services.

377

#### 378 **References:**

379 Almond, J., Sugumaar, P., Wenzel, M. N., Hill, G., & Wallis, C. (2020). Determination of the  
380 carbonyl index of polyethylene and polypropylene using specified area under band methodology with  
381 ATR-FTIR spectroscopy. *E-Polymers*, 20(1), 369-381. <https://doi.org/10.1515/epoly-2020-0041>

382

383 Almond, J., Sugumaar, P., Wenzel, M.N., Hill, G., Wallis, C., 2020. Determination of the carbonyl  
384 index of polyethylene and polypropylene using specified area under band methodology with ATR-  
385 FTIR spectroscopy. *e-Polymers* 20, 369–381. <https://doi.org/10.1515/epoly-2020-0041>

386

387 Andrade, J., Fernández-González, V., López-Mahía, P., Muniategui, S., 2019. A low-cost system to  
388 simulate environmental microplastic weathering. *Marine Pollution Bulletin* 149, 110663.  
389 <https://doi.org/10.1016/j.marpolbul.2019.110663>

390

391 Andrady, A.L., 2017. The plastic in microplastics: A review. *Marine Pollution Bulletin* 119, 12–22.  
392 <https://doi.org/10.1016/j.marpolbul.2017.01.082>

393

394 Andrady, A.L., 2015. Persistence of Plastic Litter in the Oceans, in: Bergmann, M., Gutow, L.,  
395 Klages, M. (Eds.), *Marine Anthropogenic Litter*. Springer International Publishing, Cham, pp. 57–72.  
396 [https://doi.org/10.1007/978-3-319-16510-3\\_3](https://doi.org/10.1007/978-3-319-16510-3_3)

397

398 Andrady, A.L., 2011. Microplastics in the marine environment. *Marine Pollution Bulletin* 62, 1596–  
399 1605. <https://doi.org/10.1016/j.marpolbul.2011.05.030>

400

401 Avio, C.G., Gorbi, S., Regoli, F., 2017. Plastics and microplastics in the oceans: From emerging  
402 pollutants to emerged threat. *Marine Environmental Research* 128, 2–11.  
403 <https://doi.org/10.1016/j.marenvres.2016.05.012>

404

405 Badji, C., Beigbeder, J., Garay, H., Bergeret, A., Bénézet, J.-C., Desauziers, V., 2018. Correlation  
406 between artificial and natural weathering of hemp fibers reinforced polypropylene biocomposites.  
407 *Polymer Degradation and Stability* 148, 117–131.

408 <https://doi.org/10.1016/j.polymdegradstab.2018.01.002>

409

410 Boucher, C., Morin, M., Bendell, L.I., 2016. The influence of cosmetic microbeads on the sorptive  
411 behavior of cadmium and lead within intertidal sediments: A laboratory study. *Regional Studies in*  
412 *Marine Science* 3, 1–7. <https://doi.org/10.1016/j.rsma.2015.11.009>

413

414 Bringer, A., Cachot, J., Dubillot, E., Lalot, B., Thomas, H., 2021a. Evidence of deleterious effects of  
415 microplastics from aquaculture materials on pediveliger larva settlement and oyster spat growth of  
416 Pacific oyster, *Crassostrea gigas*. *Science of The Total Environment* 794, 148708.  
417 <https://doi.org/10.1016/j.scitotenv.2021.148708>

418

419 Bringer, A., Le Floch, S., Kerstan, A., Thomas, H., 2021b. Coastal ecosystem inventory with  
420 characterization and identification of plastic contamination and additives from aquaculture materials.  
421 *Marine Pollution Bulletin* 167, 112286. <https://doi.org/10.1016/j.marpolbul.2021.112286>

422

423 Cai, L., Wang, J., Peng, J., Wu, Z., Tan, X., 2018. Observation of the degradation of three types of  
424 plastic pellets exposed to UV irradiation in three different environments. *Science of The Total*  
425 *Environment* 628–629, 740–747. <https://doi.org/10.1016/j.scitotenv.2018.02.079>

426

427 Cole, M., Lindeque, P., Fileman, E., Halsband, C., Goodhead, R., Moger, J., Galloway, T.S., 2013.  
428 Microplastic Ingestion by Zooplankton. *Environ. Sci. Technol.* 47, 6646–6655.  
429 <https://doi.org/10.1021/es400663f>

430

431 Conforto, E., Joguet, N., Buisson, P., Vendeville, J.-E., Chaigneau, C., Maugard, T., 2015. An  
432 optimized methodology to analyze biopolymer capsules by environmental scanning electron  
433 microscopy. *Materials Science and Engineering: C* 47, 357–366.  
434 <https://doi.org/10.1016/j.msec.2014.11.054>

435

436 Gerritse, J., Leslie, H.A., de Tender, C.A., Devriese, L.I., Vethaak, A.D., 2020. Fragmentation of  
437 plastic objects in a laboratory seawater microcosm. *Sci Rep* 10, 10945.  
438 <https://doi.org/10.1038/s41598-020-67927-1>  
439

440 Gewert, B., Plassmann, M., Sandblom, O., MacLeod, M., 2018. Identification of Chain Scission  
441 Products Released to Water by Plastic Exposed to Ultraviolet Light. *Environ. Sci. Technol. Lett.* 5,  
442 272–276. <https://doi.org/10.1021/acs.estlett.8b00119>  
443

444 Gewert, B., Plassmann, M.M., MacLeod, M., 2015. Pathways for degradation of plastic polymers  
445 floating in the marine environment. *Environ. Sci.: Processes Impacts* 17, 1513–1521.  
446 <https://doi.org/10.1039/C5EM00207A>  
447

448 Guo, X., Wang, J., 2019. The chemical behaviors of microplastics in marine environment: A review.  
449 *Marine Pollution Bulletin* 142, 1–14. <https://doi.org/10.1016/j.marpolbul.2019.03.019>  
450

451 Han, C., Sahle-Demessie, E., Zhao, A.Q., Richardson, T., Wang, J., 2018. Environmental aging and  
452 degradation of multiwalled carbon nanotube reinforced polypropylene. *Carbon* 129, 137–151.  
453 <https://doi.org/10.1016/j.carbon.2017.10.038>  
454

455 Hebner, T.S., Maurer-Jones, M.A., 2020. Characterizing microplastic size and morphology of  
456 photodegraded polymers placed in simulated moving water conditions. *Environ. Sci.: Processes*  
457 *Impacts* 22, 398–407. <https://doi.org/10.1039/C9EM00475K>  
458

459 Hermabessiere, L., Dehaut, A., Paul-Pont, I., Lacroix, C., Jezequel, R., Soudant, P., Duflos, G., 2017.  
460 Occurrence and effects of plastic additives on marine environments and organisms: A review.  
461 *Chemosphere* 182, 781–793. <https://doi.org/10.1016/j.chemosphere.2017.05.096>  
462

463 Holmes, L.A., Turner, A., Thompson, R.C., 2012. Adsorption of trace metals to plastic resin pellets in  
464 the marine environment. *Environmental Pollution* 160, 42–48.  
465 <https://doi.org/10.1016/j.envpol.2011.08.052>  
466

467 Julienne, F., Lagarde, F., Delorme, N., 2019. Influence of the crystalline structure on the  
468 fragmentation of weathered polyolefines. *Polymer Degradation and Stability* 170, 109012.  
469 <https://doi.org/10.1016/j.polymdegradstab.2019.109012>  
470

471 Kalogerakis, N., Karkanorachaki, K., Kalogerakis, G.C., Triantafyllidi, E.I., Gotsis, A.D.,  
472 Partsinevelos, P., Fava, F., 2017. Microplastics Generation: Onset of Fragmentation of Polyethylene  
473 Films in Marine Environment Mesocosms. *Front. Mar. Sci.* 4.  
474 <https://doi.org/10.3389/fmars.2017.00084>

475 Law, K.L., Morét-Ferguson, S., Maximenko, N.A., Proskurowski, G., Peacock, E.E., Hafner, J.,  
476 Reddy, C.M., 2010. Plastic Accumulation in the North Atlantic Subtropical Gyre. *Science* 329, 1185–  
477 1188. <https://doi.org/10.1126/science.1192321>  
478

479 León, V.M., García, I., González, E., Samper, R., Fernández-González, V., Muniategui-Lorenzo, S.,  
480 2018. Potential transfer of organic pollutants from littoral plastics debris to the marine environment.  
481 *Environmental Pollution* 236, 442–453. <https://doi.org/10.1016/j.envpol.2018.01.114>  
482

483 Leslie, H.A., van Velzen, M.J.M., Brandsma, S.H., Vethaak, A.D., Garcia-Vallejo, J.J., Lamoree,  
484 M.H., 2022. Discovery and quantification of plastic particle pollution in human blood. *Environment*  
485 *International* 163, 107199. <https://doi.org/10.1016/j.envint.2022.107199>  
486

487 Lott, C., Eich, A., Unger, B., Makarow, D., Battagliarin, G., Schlegel, K., Lasut, M.T., Weber, M.,  
488 2020. Field and mesocosm methods to test biodegradable plastic film under marine conditions. *PLoS*  
489 *ONE* 15, e0236579. <https://doi.org/10.1371/journal.pone.0236579>

490

491 Lv, Y., Huang, Y., Yang, J., Kong, M., Yang, H., Zhao, J., Li, G., 2015. Outdoor and accelerated  
492 laboratory weathering of polypropylene: A comparison and correlation study. *Polymer Degradation  
493 and Stability* 112, 145–159. <https://doi.org/10.1016/j.polyimdegradstab.2014.12.023>

494

495 Masry, M., Rossignol, S., Gardette, J.-L., Therias, S., Bussi re, P.-O., Wong-Wah-Chung, P., 2021.  
496 Characteristics, fate, and impact of marine plastic debris exposed to sunlight: A review. *Marine  
497 Pollution Bulletin* 171, 112701. <https://doi.org/10.1016/j.marpolbul.2021.112701>

498

499 Paluselli, A., Fauvelle, V., Galgani, F., Semp r , R., 2019. Phthalate Release from Plastic Fragments  
500 and Degradation in Seawater. *Environ. Sci. Technol.* 53, 166–175.  
501 <https://doi.org/10.1021/acs.est.8b05083>

502

503 Prata, J.C., da Costa, J.P., Lopes, I., Duarte, A.C., Rocha-Santos, T., 2020. Environmental exposure to  
504 microplastics: An overview on possible human health effects. *Science of The Total Environment* 702,  
505 134455. <https://doi.org/10.1016/j.scitotenv.2019.134455>

506

507 Rajakumar, K., Sarasvathy, V., Thamarai Chelvan, A., Chitra, R., Vijayakumar, C.T., 2009. Natural  
508 Weathering Studies of Polypropylene. *J Polym Environ* 17, 191–202. [https://doi.org/10.1007/s10924-  
509 009-0138-7](https://doi.org/10.1007/s10924-009-0138-7)

510

511 Rani, M., Shim, W.J., Han, G.M., Jang, M., Al-Odaini, N.A., Song, Y.K., Hong, S.H., 2015.  
512 Qualitative Analysis of Additives in Plastic Marine Debris and Its New Products. *Arch Environ  
513 Contam Toxicol* 69, 352–366. <https://doi.org/10.1007/s00244-015-0224-x>

514

515 Ranjan, V.P., Goel, S., 2019. Degradation of Low-Density Polyethylene Film Exposed to UV  
516 Radiation in Four Environments. *J. Hazard. Toxic Radioact. Waste* 23, 04019015.  
517 [https://doi.org/10.1061/\(ASCE\)HZ.2153-5515.0000453](https://doi.org/10.1061/(ASCE)HZ.2153-5515.0000453)  
518

519 Singh, B., Sharma, N., 2008. Mechanistic implications of plastic degradation. *Polymer Degradation*  
520 *and Stability* 93, 561–584. <https://doi.org/10.1016/j.polymdegradstab.2007.11.008>  
521

522 Song, Y.K., Hong, S.H., Jang, M., Han, G.M., Jung, S.W., Shim, W.J., 2017. Combined Effects of UV  
523 Exposure Duration and Mechanical Abrasion on Microplastic Fragmentation by Polymer Type.  
524 *Environ. Sci. Technol.* 51, 4368–4376. <https://doi.org/10.1021/acs.est.6b06155>  
525

526 Tang, C.-C., Chen, H.-I., Brimblecombe, P., Lee, C.-L., 2019. Morphology and chemical properties of  
527 polypropylene pellets degraded in simulated terrestrial and marine environments. *Marine Pollution*  
528 *Bulletin* 149, 110626. <https://doi.org/10.1016/j.marpolbul.2019.110626>  
529

530 Wang, J., Tan, Z., Peng, J., Qiu, Q., Li, M., 2016. The behaviors of microplastics in the marine  
531 environment. *Marine Environmental Research* 113, 7–17.  
532 <https://doi.org/10.1016/j.marenvres.2015.10.014>  
533

534 Wang, T., Wang, L., Chen, Q., Kalogerakis, N., Ji, R., Ma, Y., 2020. Interactions between  
535 microplastics and organic pollutants: Effects on toxicity, bioaccumulation, degradation, and transport.  
536 *Science of The Total Environment* 748, 142427. <https://doi.org/10.1016/j.scitotenv.2020.142427>  
537

538 Yang, X., Ding, X., 2006. Prediction of outdoor weathering performance of polypropylene filaments  
539 by accelerated weathering tests. *Geotextiles and Geomembranes* 24, 103–109.  
540 <https://doi.org/10.1016/j.geotextmem.2005.11.002>  
541

542 Zettler, E.R., Mincer, T.J., Amaral-Zettler, L.A., 2013. Life in the “Plastisphere”: Microbial  
543 Communities on Plastic Marine Debris. *Environ. Sci. Technol.* 47, 7137–7146.  
544 <https://doi.org/10.1021/es401288x>

545

546 Zhang, N., Li, Y.B., He, H.R., Zhang, J.F., Ma, G.S., 2021. You are what you eat: Microplastics in the  
547 feces of young men living in Beijing. *Science of The Total Environment* 767, 144345.  
548 <https://doi.org/10.1016/j.scitotenv.2020.144345>

549